Scattering by ionization and phonon emission in semiconductors

R. C. Alig, S. Bloom, and C. W. Struck
RCA Laboratories, Princeton, New Jersey 08540
(Received 8 May 1980)

Calculations of the pair-creation energy ϵ, the Fano factor F, and the quantum yield for semiconductors are done for the assumptions that in each scattering event all possible sets of product particles are equally probable, that the energy bands are those of free particles separated by a band gap E_g, and that there is a single phonon energy $\hbar\omega_0$. A new method of calculating these quantities is advanced. In it a pair-number probability distribution $p_n(E)$, the probability that a particle with energy E ultimately creates n pairs, is calculated recursively with increasing E. The first and second moments of the $p_n(E)$ distribution yield ϵ, F, and the quantum yield as functions of $\hbar\omega_0$, E_g, and a parameter A, proportional to the ratio of the matrix elements for electron scattering by phonon emission and by ionization. We find that a single value of A, which fits the ϵ observed for Si, gives values for these quantities in good accord with experiments for many semiconductors. The calculated ϵ is found insensitive in many semiconductors to electron-energy loss to plasmons and to differences in the threshold energy for ionization representing real band-structure features. The assumption that all possible sets of product particles are equally probable in each scattering event leads to ultimate nonuniform population of the states with energies below the threshold for ionization, in contrast to the uniform population assumed in some earlier approaches. Results of other existing approaches in which the final-state distribution is calculated, an alternate method, were duplicated using this new method. A simple paradigm is used to illustrate these methods and assumptions.

I. INTRODUCTION

A. Concept

When a particle of high kinetic energy traverses a semiconductor it scatters by ionization and by phonon emission, producing a cascade of hole-electron pairs and phonons. The number of pairs can be measured and the average energy ϵ required to create a pair obtained. Because of phonon emission, ϵ exceeds the band gap E_g of the semiconductor. In this paper, the calculation of ϵ is reviewed and a new calculation is presented.

The pair-creation energy ϵ is important in the efficiency of cathode-ray phosphors[1,2] where each emitted photon requires at least one hole-electron pair. It is also important for gamma-ray detectors, where ϵ links the charge measured in the detector to the energy of the incident gamma ray.[3,4] It has also been applied to the understanding of the secondary-electron-emission ratio.[5,6]

Experimental values of ϵ for Si and Ge were obtained in 1953 by McKay and McAfee.[7] Lappe[8] observed somewhat later that ϵ is approximately $3E_g$ in several semiconductors.

Two approaches have been introduced to calculate ϵ. The first, called here the "assumption of uniform population," was set forth by Shockley.[9] In it, it is assumed that a threshold energy E_{th} exists below which no pairs can be created and that for large incident-particle energy all states below E_{th} are ultimately populated uniformly. The second, called here the "scattering rate assumption," was used by van Roosbroeck,[10] Antoncik,[11] and Drummond and Moll.[12] In it, each scattering event creates all possible sets of three product particles with equal probability. The scattering-rate assumption allows calculation of the populations of the states below E_{th}, and *nonuniform* populations are found. Because the subthreshold populations should be calculated from the individual scattering events, and because the scattering-rate assumption gives nonunifrom subthreshold populations, we adopt here the scattering-rate assumption.

Nevertheless, the assumption of uniform population has been popular because the expression for ϵ is easily derived and is of simple form. The average energy E_K lost to the lattice by a final particle is the average energy of the subthreshold states. In the free-particle approximation this average energy is $E_K = 3E_{th}/5$. The energy required to create a hole-electron pair is then twice this loss plus the band gap: $\epsilon = \frac{6}{5}E_{th} + E_g$. Klein[13] observed that when E_{th} is chosen as $3E_g/2$, $\epsilon = 2.8E_g$, close to the observed[13,14] correlation found in many semiconductors, $\epsilon = 2.73E_g + E_r$, where $E_r \sim 0.5$ eV. This choice of E_{th} follows from conservation of both energy and momentum[15] during the scattering event. Klein also states that impact ionization experiments point to this value of E_{th} as the "most appropriate." The quantity E_r is ascribed to the superthreshold phonon losses.

In contrast, the scattering-rate assumption is mathematically difficult to use. Van Roosbroeck[10] used an analysis verified by a Monte Carlo calculation, in what he called "crazy carpentry," and was the first to obtain a nonuniform distribution of the final states. Drummond and Moll[12] used the Si band structure of Kane[16] to obtain ϵ for Si without adjustable parameters. They also show a nonuniform final-state distribution. However, their ϵ

was not close to the measured value. Here we give an improved derivation of ϵ, use the free-particle band structure, and obtain ϵ as a function of the band gap E_g, the phonon energy $\hbar\omega_0$, and a parameter A, proportional to the ratio of the mean free path for pair creation to that for phonon emission. We then get good accord with the measured ϵ for many semiconductors.

The exact calculation of the rate of scattering by ionization, i.e., by pair creation, is exceedingly expensive and so we utilize Kane's random-k approximation.[17] In this approximation, the influence of momentum conservation on the scattering rate is not apparent. We propose that momentum conservation is manifested mainly in the threshold energy E_{th}, below which the ionization scattering rate is zero. Calculations were done here for two values of the threshold energy as described in Sec. II D. We find ϵ to be insensitive to these values except for semiconductors in which scattering by phonon emission is very weak, and there are few experimental data for such semiconductors.

The calculated ϵ values depend upon whether plasmons are included in the model. Plasmon excitation was suggested for semiconductors by Zareba[18] and others,[19] following Pines[20] who showed this process to be the dominant loss mechanism for high-energy particles in metals. Plasmons are collective electron excitations with energy $\hbar\omega_p$ between 10 and 25 eV. Rothwarf[1] calculated ϵ assuming plasmon excitation. In his picture a high-energy particle creates plasmons without loss. The plasmon then decays into an electron and a hole of equal energy, as required by momentum conservation at $k=0$; the hole and electron both may form additional pairs. We consider in Sec. II E both this case and also the case that plasmon decay requires energy conservation only. We find ϵ insensitive to the presence of plasmons except for very small $\hbar\omega_p/E_g$ ratios, a condition for which there are few experimental data.

In our approach, the pair-creation energy ϵ is obtained by a new "probability method" which is described qualitatively in Sec. I B and mathematically in Sec. II.

B. Approach

The band structure above and below the energy gap is taken to be that of the free-particle model, and the optical-phonon energy $\hbar\omega_0$ is taken to be constant. The rates of scattering by pair generation $r(E)$ and by phonon generation $r'(E)$ are defined in accord with the "golden rule" of quantum mechanics. Each of these rates contains a matrix element of the scattering interaction, and the squared ratio of these matrix elements is included in an empirical constant A.

Two probability distributions are used. One, $P_m(E)$ is the probability that a particle of energy E generates exactly m phonons before scattering by ionization. The other, $p_n(E)$, is the probability that a particle of energy E ultimately creates exactly n pairs. The probability, $p_0(E)$, that a particle of energy E thermalizes without any pair production is obtained from the $P_m(E)$. The probabilities $p_n(E)$ are obtained from $p_0(E)$ by a recursion formula.

From the $p_n(E)$, the first and second moments are

$$\langle n(E)\rangle = \sum_{n=0}^{\infty} n p_n(E)\,, \tag{1}$$

$$\langle n^2(E)\rangle = \sum_{n=0}^{\infty} n^2 p_n(E)\,. \tag{2}$$

These moments give the average pair-creation energy ϵ and the Fano factor[21,22,23] F, a measure of the width of the distribution, as

$$\epsilon = E/\langle n\rangle \tag{3}$$

and

$$F = (\langle n^2\rangle - \langle n\rangle^2)/\langle n\rangle\,. \tag{4}$$

If, in an ensemble of primary particles of energy E, the number which yields n pairs is plotted versus n, this distribution peaks at $n=E/\epsilon$ and, if it were Gaussian, would have the width $[(8FE\ln 2)/\epsilon]^{1/2}$ at half-height.

The quantities $\langle n\rangle$ and $\langle n^2\rangle$, or ϵ and F, are measured most directly in experiments, such as gamma-ray detection,[22,23] which display the $p_n(E)$ distribution. These experiments are done with very large initial particle energies and give the asymptotic values $\epsilon=\epsilon(\infty)$ and $F=F(\infty)$. However, as described in Sec. III B, for photon or low-energy-electron excitation, quantum-yield measurements give $\langle n(E)\rangle$, where E is measured from the conduction-band minimum. For E large, $\langle n(E)\rangle$ is expected to be linear in E. As will be seen, the experimental data establish this linearity for energies above a few times E_g. Thus the $p_n(E)$ distribution needs to be evaluated only for energies up to a few times E_g.

In contrast to the probability method introduced here, a different method, called here the "final-state method," was used in some earlier work.[10,12] A function, denoted $L(E',E)$ here, namely the final-state distribution function, was calculated; $L(E',E)dE'$ is the fraction of thermalized particles in the ensemble of cascades initiated by primary particles of energy E which have occupied a state with energy between E' and $E'+dE'$ immediately following an ionization event and have subsequently thermalized entirely by phonon emission. Because

of the importance of $L(E', E)$ in the literature, the procedure for its exact calculation will be given in Sec. II F. Inasmuch as $L(E', E)$ cannot be measured, it will not be calculated here. Drummond and Moll[12] did calculate $L(E', E)$ and we have reproduced their results, as shown in Sec. IV A.

A diagram depicting a representative cascade is shown in Fig. 1. The equations that describe the scattering rates in cascades like this are given in Sec. II; calculations using these equations are discussed in Sec. III; and the results of these calculations are discussed in Sec. IV.

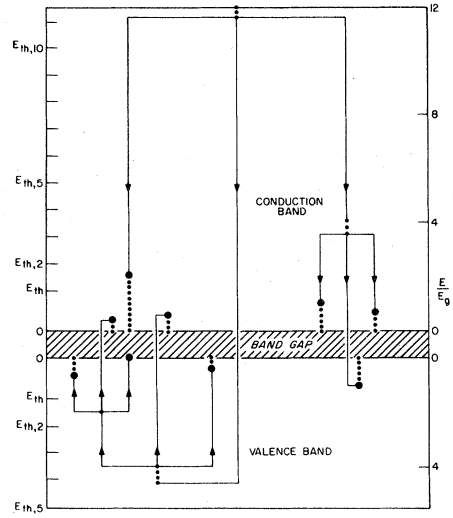

FIG. 1. Diagram of a representative cascade. The kinetic energy of particles, represented by dots, is plotted vertically, increasing upward from the conduction-band edge for electrons and increasing downward from the valence-band edge for holes. This energy is shown in units of E_g at right, and the energy thresholds for ionization are shown at left. No meaning is assigned to the horizontal direction. The phonon energy is $0.2E_g$ and phonon scattering events are indicated by connected dots separated vertically by this energy. Ionization scattering events are indicated by three lines originating on a dot. Each line terminates on a dot representing one of the scattered particles. The center line is drawn to the particle with charge opposite to that of the scattered particle. The arrows indicate the direction of the cascade. This cascade originated with an electron having $12E_g$ of kinetic energy and resulted in four pairs; cascades resulting in four pairs would occur with probability $p_4(12E_g)$. In this cascade two phonons are created before the first pair creation; cascades with two phonons created before the first pair creation would occur with probability $P_2(12E_g)$. The large dots are final-state particles whose normalized distribution function is $L(E', 12E_g)$, where E' is the ordinate of the large dot. If an experiment were to consist entirely of two primary particles, one of which is the origin of this cascade and the other of which is the origin of a cascade resulting in six pairs, then $\epsilon = (12+12)E_g/(4+6) = 2.4E_g$, *not* $2.5E_g$ obtained by averaging the average cascade-pair-creation energies of $3E_g$ and $2E_g$.

C. Two-level approximation

Before considering the general theory and calculations, we give here a simple model, called the "two-level approximation," as a useful paradigm. In this paradigm, particles above the threshold energy E_{th} are assumed to lose energy only by pair generation; particles below E_{th} lose energy only by phonon generation. We assume further that there are two states near E_{th} with energies $E_{th} \pm \delta$ where δ is small and that all particles in the pair cascade pass through one of these two states. Since the two states are nearly equal in energy, they are occupied with equal probability.

Particles in the state $E_{th} - \delta$ are final-state particles, decay further only by phonon generation, and generate E_{th} in phonon energy. Particles in the state $E_{th} + \delta$ create one more pair, yield three final-state particles with energy $(E_{th} - E_g)/3$,[15] and generate, in total, $E_{th} - E_g$ in phonon energy. The states with energies $(E_{th} - E_g)/3$ and $E_{th} - \delta$ are the only two possible final states and the lower-energy state is populated with three times as many particles as the higher-energy state. Thus the distribution of the final states is *not* uniform.

The average energy E_K generated in phonons for each final particle, i.e., the average energy of the final states, is $[E_{th} + (E_{th} - E_g)]/4 = \frac{1}{2}E_{th} - \frac{1}{4}E_g$. The average energy required for each final pair is $\epsilon = 2E_K + E_g = E_{th} + \frac{1}{2}E_g$. This particular analysis exemplifies the final-state method discussed in Sec. II F.

More particularly, in Sec. II F, E_K is calculated using the distribution function, $L(E', E)$, describing particles in the final states E'. We have just seen that one-quarter of the final-state particles have energy $\sim E_{th}$ and three-quarters have energy $(E_{th} - E_g)/3$. Thus

$$d(E') \equiv \lim_{E \to \infty} L(E', E) = \tfrac{1}{4}\delta(E' - E_{th}) + \tfrac{3}{4}\delta[E' - \tfrac{1}{3}(E_{th} - E_g)] .$$

The average loss per final particle is

$$E_K = \int_0^\infty E' d(E') dE' = \tfrac{1}{2}E_{th} - \tfrac{1}{4}E_g$$

and $\epsilon = E_{th} + \frac{1}{2}E_g$, as found above.

We now address this problem according to our probability method. A particle of energy $E \gg E_{th}$ initiates a cascade resulting in, for example, t pairs, that is, $2t + 1$ particles distributed in the two levels near E_{th}. In this cascade, t units of E_g are expended. Thus, using $2t + 1 \approx 2t$, energy conservation requires $E - tE_g = 2tE_{th}$ and therefore $t \approx E/(2E_{th} + E_g)$. A number, s, of these $2t$ particles will

be in the state at $E_{th}+\delta$, with probability given by the binomial distribution, $B_{2t}(s)=\binom{2t}{s}2^{-2t}$. This bibinomial distribution has the moments $\sum_{s=0}^{2t}B_{2t}(s)=1$, $\langle s\rangle=t$, and $\langle s^2\rangle=t(t+\frac{1}{2})$. The s particles in the state $E_{th}+\delta$ produce s additional pairs for a total of $t+s$ pairs. Thus the distribution function $p_n(E)$ is $p_{t+s}(E)=B_{2t}(s)$. Using Eq. (1), $\langle n\rangle=\sum_{s=0}^{2t}(t+s)B_{2t}(s)=2t$; from Eq. (3), $\epsilon=E_{th}+\frac{1}{2}E_g$.

A value of F can be calculated using the $p_{t+s}(E)$ distribution of the two-level approximation. Using Eq. (2), $\langle n^2\rangle=\sum_{s=0}^{2t}(t+s)^2B_{2t}(s)=4t^2+\frac{1}{2}t$, and, from Eq. (4), $F=\frac{1}{4}$ (Ref. 24). These analyses exemplify the new probability method set forth in Sec. II A.

In this paper we use $E_{th}=E_g$ and $E_{th}=3E_g/2$. The ϵ's predicted for the two-level approximation are then $3E_g/2$ and $2E_g$, respectively. Similarly, the free-particle model used here gives values of ϵ dependent upon E_{th}. However, when phonon scattering above E_{th} is included, this difference in the ϵ values decreases and is very small for strong phonon scattering. The F values calculated for the two-level approximation and for the free-particle model are insensitive to E_{th}.

II. THEORY

A. Model equations

In this section formulas for the rates at which a particle is scattered by either phonon emission or by ionization are derived and then used to construct the probability functions $p_n(E)$.

The rate at which a particle of energy E scatters by ionization is, by the golden rule,

$$r(E)=\frac{2\pi}{\hbar}\sum_j|H_j|^2\delta(E-E_j-E_g)\,, \tag{5}$$

where H_j is the matrix element of the Coulomb interaction.[17] The index j denotes the states of the recoil particle, the new electron, and the new hole. The energy E_j is the sum of the kinetic energies of these three particles. All phonon generation accompanying the ionization event is ignored in the use of Eq. (5).

Likewise, the rate at which the particle of energy E scatters by emission of a phonon of energy $\hbar\omega_0$ is

$$r'(E)=\frac{2\pi}{\hbar}\sum_j|H_j'|^2\delta(E-E_j-\hbar\omega_0)\,, \tag{6}$$

where H_j' is the matrix element of the electron-phonon interaction. Here j denotes the states of the recoil particle and the phonons, and E_j is the kinetic energy of the recoil particle.

The probability that a particle of energy E scatters first by ionization is[12]

$$P_0(E)=r(E)/[r(E)+r'(E)]\,, \tag{7}$$

and $1-P_0(E)$ is the probability that the particle of energy E scatters first by phonon emission. Thus the probability that a particle scatters by ionization after creating just one phonon is

$$P_1(E)=[1-P_0(E)]\,P_0(E-\hbar\omega_0)\,, \tag{8}$$

and the probability that it scatters by ionization after creating m phonons is

$$P_m(E)=[1-P_0(E)]\,P_{m-1}(E-\hbar\omega_0)\,. \tag{9}$$

Applying this recursion formula m times, one has[25]

$$P_m(E)=P_0(E-m\hbar\omega_0)\prod_{i=0}^{m-1}[1-P_0(E-i\hbar\omega_0)]\,. \tag{10}$$

The $P_m(E)$ distribution does not sum to unity. The remnant is $p_0(E)$, the probability that a particle of energy E decays to zero kinetic energy without scattering by ionization,[12]

$$p_0(E)=1-\sum_{m=0}^{\infty}P_m(E)\,. \tag{11}$$

In Eq. (11), $P_m(E)$ is zero for $m>(E-E_{th})/\hbar\omega_0$, from Eq. (10).

B. The probability method

We are now in a position to develop the pair-number probability distribution $p_n(E)$ central to our probability method. The probability $p_n(E)$ that a primary particle of energy E will be the origin of a cascade containing n and only n ionization events is equal to the sum of two products: the probability, $P_0(E)$, that the primary particle will ionize first before producing phonons, times the probability, $r_{n-1}(E)/r(E)$, that the three-product particles will cause a total of $n-1$ ionizations, plus the probability, $1-P_0(E)$, that the primary particle first creates a phonon, times the probability, $p_n(E-\hbar\omega_0)$, that this particle—which is now at energy $E-\hbar\omega_0$—will be the origin of a cascade containing the n ionizations. Thus

$$p_n(E)=P_0(E)\frac{r_{n-1}(E)}{r(E)}+[1-P_0(E)]\,p_n(E-\hbar\omega_0)\,,\quad n\geq 1 \tag{12}$$

is the resulting recursion relation. Here $r_{n-1}(E)$ is the ionization rate of Eq. (5) but reduced by the probability that the three product particles will lead to the total of $n-1$ further ionizations:

$$r_{n-1}(E)=\frac{2\pi}{\hbar}\sum_{f,e,h}\sum_{i,j,k}|H_{feh}|^2p_i(E_f)p_j(E_e)p_k(E_h)\times\delta(E-E_f-E_e-E_h-E_g)\,, \tag{13}$$

where the subscripts f, e, and h denote the recoil particle and the newly created electron and hole, and i, j, and k are non-negative integers such that $i+j+k=n-1$. For example, if the particle of energy E results in only one ionization event, then

$$r_0(E) = \frac{2\pi}{\hbar} \sum_{f,e,h} |H_{feh}|^2 p_0(E_f) p_0(E_e) p_0(E_h) \times \delta(E - E_f - E_e - E_h - E_g) . \quad (14)$$

C. Assumptions

The scattering-rate assumption, i.e., equal probabilities for occupation of all allowed states in each scattering event, means that all the nonzero H_j in Eq. (5) are identical and that all nonzero H_j' in Eq. (6) are identical. Since the energy $\hbar\omega_0$ of all the phonon states is assumed to be the same,

$$r'(E) = \frac{2\pi}{\hbar} |M'|^2 \sum_j \delta(E - E_j - \hbar\omega_0) = \frac{2\pi}{\hbar} |M'|^2 \rho(E - \hbar\omega_0) , \quad (15)$$

where $|M'|^2 = |H_j'|^2$ and

$$\rho(E) = (V/2\pi^2)(2m/\hbar^2)^{3/2} E^{1/2} \quad (16)$$

is the density of states in the free-particle model in which the band structure is parabolic and isotropic. Here V is the semiconductor volume and m is the free-particle mass.

Because the free-particle band structure is parabolic, the selection of the H_j which are nonzero because of momentum conservation is not trivial. However, it is clear that H_j is 0 when $E < E_{th}$. Above E_{th} the random-k approximation of Kane[17,26] was used to evaluate $r(E)$, i.e.,

$$r(E) = \frac{2\pi}{\hbar} \frac{\Delta}{V} |M|^2 \int dE_f \int dE_e \int dE_h \rho(E_f)\rho(E_e)\rho(E_h) \delta(E - E_f - E_e - E_h - E_g) \quad \text{for } E \geq E_{th},$$
$$r(E) = 0 \quad \text{for } E < E_{th}, \quad (17)$$

where $|M|^2 = |H_j|^2$ for all j and Δ is the atomic volume per electronic state. Then,[27] using Eq. (16),

$$r(E) = \frac{2\pi}{\hbar} |M|^2 \frac{V^2\Delta}{8\pi^6} \left(\frac{2m}{\hbar^2}\right)^{9/2} \frac{2\pi(E - E_g)^{7/2}}{105} \quad \text{for } E > E_{th}, \quad (18)$$

that is, the rate $r(E)$ in Eq. (18) rises smoothly from zero when $E_{th} = E_g$ but rises abruptly from zero to a nonzero value at E_{th} when $E_{th} > E_g$. Likewise, in the calculation of $r_{n-1}(E)$, $r_{n-1}(E) = 0$ for $E < E_{th,n}$ where $E_{th,n}$ is the threshold energy for a cascade containing n ionization events, and for $E \geq E_{th,n}$,

$$r_{n-1}(E) = \frac{2\pi}{\hbar} \frac{\Delta}{V} |M|^2 \sum_{i,j} \int dE_f \int dE_e \int dE_h \rho(E_f)\rho(E_e)\rho(E_h) p_i(E_f) p_j(E_e) p_{n-1-i-j}(E_h) \delta(E - E_f - E_e - E_h - E_g) . \quad (19)$$

The calculation of $p_n(E)$ then requires only the ratio of Eqs. (15) and (18), i.e.,

$$\frac{r'(E)}{r(E)} = A \frac{105}{2\pi} \frac{(E - \hbar\omega_0)^{1/2}}{(E - E_g)^{7/2}} , \quad (20)$$

where the parameter A is

$$A \equiv \frac{|M'|^2}{|M|^2} \frac{4\pi^4}{V\Delta} \left(\frac{\hbar^2}{2m}\right)^3 . \quad (21)$$

This parameter is the one adjustable constant of the calculation; it will be assumed independent of the particle energy and invariant for electrons and holes, for different materials, and for all ambient conditions.

D. Threshold values

The literature is obscure about the necessity for including momentum conservation in the calculation of ϵ. Using the assumption of uniform population,[9,13] momentum conservation is essential for accord between theory and experiment. If momentum conservation is ignored, $E_{th} = E_g$ and $\epsilon = 6E_{th}/5 + E_g = 2.2E_g$, far from the slope of 2.73. On the other hand, van Roosbroeck,[10] Drummond and Moll,[12] and others use the scattering-rate assumption and do not discuss momentum conservation explicitly in calculating ϵ.

Momentum is certainly conserved in ionization scattering: See, for example, recent measurements of impact ionization.[28] For the free-particle model with momentum conservation, one can then obtain[29] thresholds $E_{th,n}$ for creating n pairs:

$$E_{th} \equiv E_{th,1} = 3E_g/2 ,$$
$$E_{th,n} = 5E_{th,n-1} + 2E_g - 4(E_{th,n-1}^2 + \tfrac{1}{2} E_g E_{th,n-1})^{1/2} = E_{th,n-1} + E_g + E_g^2/8E_{th,n-1} + \cdots \quad \text{for } n \geq 2 . \quad (22)$$

However, there may be phenomena in the semiconductor, e.g., band-structure complexities or phonon creation accompanying the pair-creation event, which these thresholds do not describe. We believe that these phenomena are describable, at least roughly, by the free-particle picture if the thresholds are lowered toward those for energy conservation only:

$$\overline{E}_{th} \equiv \overline{E}_{th,1} = E_g \,, \qquad \overline{E}_{th,n} = \overline{E}_{th,n-1} + E_g \quad \text{for } n \geq 2 \,. \tag{23}$$

These phenomena will be described here using Eq. (23), that is, by neglecting momentum conservation in the free-particle model. The values of ϵ calculated with Eq. (23) will be overscored; those calculated with Eq. (22) will be unmarked.

E. Plasmons

All semiconductor materials exhibit[20] a characteristic plasmon energy $\hbar\omega_p$ that generally exceeds the band gap, and it is generally believed that a particle with energy much greater than $\hbar\omega_p$ dissipates most of its energy into plasmons.[1,18,19] In considering plasmons we assume that a high-energy primary particle deposits all its energy into plasmons without loss. The cascade of particles and phonons from the primary particle is then the aggregate of the small cascades originating with the plasmons. If the plasmon energy is a large multiple of the band gap, then the small cascade will appear similar to a cascade originating with a particle of the plasmon energy. For these energies, ϵ is expected to be independent of the energy as indicated by the linearity in energy of the quantum yield. Therefore the value of ϵ calculated for a small cascade will be very close to the value of ϵ calculated for the cascade produced by the primary particle in the absence of plasmons. However, if the plasmon energy is only slightly larger than the band-gap energy, as may be the case in SiO_2,[30] the intervention of plasmons in the cascade could change the average pair-creation energy significantly.

If energy is assumed to be deposited into plasmons, then it must be determined whether momentum is explicitly conserved in the plasmon decay. Rothwarf[1] assumes momentum is conserved and decay occurs only from the zero-momentum state. However, there may be phenomena, as described in the preceding section, which cause the decay to appear to occur with only energy conservation. We calculate both cases here. The ϵ for plasmons decaying with momentum conservation are labeled ϵ_k; those decaying with energy conservation only are labeled $\epsilon_{\overline{k}}$. The ϵ can also be overscored or not to denote, as in Sec. II D, the threshold energy used to describe ionization.

If momentum is conserved in the plasmon decay, then each plasmon produces two particles of energy $E^*/2$ where $E^* = \hbar\omega_p - E_g$. Then, by analogy to Eq. (3), the pair-creation energy is

$$\epsilon_k(\hbar\omega_p) = \hbar\omega_p / [2\langle n(E^*/2)\rangle + 1] \,, \tag{24}$$

where the denominator is the average number of pairs created by the plasmon and $\langle n(E^*/2)\rangle$ is given by Eq. (1).

If momentum is not conserved, then

$$\epsilon_{\overline{k}}(\hbar\omega_p) = \hbar\omega_p / \langle J(\hbar\omega_p)\rangle \,, \tag{25}$$

where $\langle J(\hbar\omega_p)\rangle$, the average number of pairs created by the plasmon, is given by

$$\langle J(\hbar\omega_p)\rangle = 1 + \frac{\int_0^{E^*} \sum_{n=0}^{\infty} n \sum_{m=0}^{n} p_m(E') p_{n-m}(E^* - E') \rho(E') \rho(E^* - E') dE'}{\int_0^{E^*} \rho(E') \rho(E^* - E') dE'} = 1 + 2 \frac{\int_0^{E^*} \langle n(E')\rangle \rho(E') \rho(E^* - E') dE'}{\int_0^{E^*} \rho(E') \rho(E^* - E') dE'} \,, \tag{26}$$

with $p_n(E)$ given by Eq. (12) and $\rho(E)$ by Eq. (16).[31]

From Eqs. (24) and (25) these pair-creation energies have the limits for large arguments $\epsilon \equiv \epsilon(\infty) = \epsilon_k(\infty) = \epsilon_{\overline{k}}(\infty)$ and $\overline{\epsilon} \equiv \overline{\epsilon}(\infty) = \overline{\epsilon}_k(\infty) = \overline{\epsilon}_{\overline{k}}(\infty)$. These identities reflect the fact that in this limit the two particles created by the plasmon are formed dominantly at energies E where $\epsilon(E)$ or $\overline{\epsilon}(E)$ is constant.

F. Final-state method

The final-state distribution function $L(E', E)$ described in the Introduction and utilized in previous treatments is

$$L(E', E) = N(E', E)/N(E) \,, \tag{27}$$

where

$$N(E) = \int_0^E N(E', E) dE' \tag{28}$$

and $N(E', E)dE'$ is the average, over an ensemble of cascades originating from primary particles of energy E, of the number of particles which arrive at a state with energy between E' and $E' + dE'$ as a direct result of an ionization event and which decay from E' entirely by phonon emission.

The $N(E', E)$ can be calculated as

$$N(E', E) = p_0(E)\,\delta(E', E) + \sum_{m=0}^{\infty} P_m(E) \frac{S(E', E - m\hbar\omega_0)}{r(E - m\hbar\omega_0)} \,, \tag{29}$$

where

$$S(E', E - m\hbar\omega_0) = \int dE_e \int dE_h \int dE_f \rho(E_e)\rho(E_h)\rho(E_f)\,\delta(E - m\hbar\omega_0 - E_g - E_e - E_h - E_f) \times [N(E', E_e) + N(E', E_h) + N(E', E_f)]\,, \tag{30}$$

and $p_0(E)$, $P_m(E)$, $r(E - m\hbar\omega_0)$, and $\rho(E)$ are defined in Eqs. (11), (10), (18), and (16), respectively. That is, in Eq. (29), $N(E', E)$ for an ensemble of primary particles at energy E is expressed in terms of the $N(E', E'')$ for the three products of the first ionization event of the primary particle. The first term on the right-hand side of Eq. (29) is the fraction of the primary particles which never scatter by ionization. The second term is the average number of final-state particles at E' created by the hole and the electron and recoil particle from this first ionization event. This first ionization event occurs with probability $P_m(E)$ only after the primary particle has created m phonons and has lost $m\hbar\omega_0$ in energy.

Equation (29) is a recursion formula defining $N(E', E)$ in terms of $N(E', E'')$ for $E'' < E$. This recursion formula is initiated with the values

$$N(E', E) = \delta(E', E) \tag{31}$$

for $E < E_{th}$. One recognizes, by similarity of definition, that $N(E)$ satisfies

$$N(E) = 1 + 2\langle n(E)\rangle\,, \tag{32}$$

where $\langle n(E)\rangle$ is given by Eq. (1). Thus Eq. (28) is an alternate calculation of $\langle n(E)\rangle$ and, through Eq. (3), of ϵ. We are, however, unable to find a procedure for calculating $\langle n^2(E)\rangle$ using the final-state method.[24]

The function $L(E', E)$ for $E \to \infty$ is the $d(E')$ of Ref. (12).[32] For the assumption of uniform population, it is zero for $E' > E_{th}$ and is $\frac{3}{2}(E'/E_{th}^3)^{1/2}$ for $E' \leq E_{th}$.

III. CALCULATIONS

A. Pair-creation energies

The calculations were done by computer[33] for specific values of E_g and $\hbar\omega_0$. Each function of energy was expressed as a table for $E_{th} \leq E \leq 16E_g$ in steps of $\hbar\omega_0$. For a specified value of A in Eq. (20), the function $P_0(E)$ was calculated. Then Eq. (10) was used to obtain the functions $P_m(E)$ and Eq. (11) to obtain $p_0(E)$. The functions $p_n(E)$ for $1 \leq n \leq 7$ were calculated using Eqs. (12) and (19); the double integration required to obtain $r_{n-1}(E)$ was done using Simpson's rule. Finally $\epsilon(E)$ was calculated using Eqs. (1) and (3).

The values of E_g and $\hbar\omega_0$ for each semiconductor are shown in Table I, together with measured values of ϵ taken from the literature. The band gap was chosen to be the smallest of the direct and indirect gaps. Since energy losses in phonon scattering are believed to be due to the long-wavelength longitudinal-optical phonon,[34] this value was chosen for $\hbar\omega_0$.

The values of E_g and $\hbar\omega_0$ for Si were used in the initial calculations. Figure 2 shows calculated values of $\epsilon(E)$ and $\bar{\epsilon}(E)$ for $A = 0$ and 5.2 eV^3. For $A = 0$, $\epsilon = E$ for $E_{th} \leq E \leq E_{th,2}$ and $\bar{\epsilon} = E$ for $\bar{E}_{th} \leq E \leq \bar{E}_{th,2}$, since a particle with energy in this range scatters once and only once by ionization. For large E, $\epsilon(E)$ and $\bar{\epsilon}(E)$ approach constant values ϵ and $\bar{\epsilon}$. For $A \neq 0$, $\epsilon(E)$ and $\bar{\epsilon}(E)$ become large as E decreases toward the threshold energy due to the strong competition of scattering by phonon emission at low energies. For the value $A = 5.2$ eV^3, $\epsilon(E)$ and $\bar{\epsilon}(E)$ are indistinguishable within and above the energy range shown here, and they approach a constant value $\epsilon = \bar{\epsilon}$ for large E.

Figure 3 shows the asymptotic values ϵ and $\bar{\epsilon}$ plotted versus A for Si; the values at $A = 0$ and 5.2 eV^3 are identical to those approached in Fig. 2. A difference in the values of ϵ and $\bar{\epsilon}$ at $A = 0$ is expected from the two-level approximation and the convergence of the values at large A is expected from the dominance of scattering by phonon emission. The value of A at which the convergence of ϵ and $\bar{\epsilon}$ occurs, seen to be approximately 0.1 eV^3 in Fig. 3 for Si, varies with E_g and $\hbar\omega_0$.

The ratio $r'(E)/r(E)$, defined in Eq. (20), is the ratio l_i/l_p of the mean free paths for electron scattering by ionization and by phonon emission.[16] At $E = 5$ eV in Si the aforementioned value $A = 0.1$ eV^3 implies $l_i/l_p = 0.03$. There have been a number of studies[35] of Si from which values of l_i/l_p for $E = 5$ eV have been inferred. While these values are widely scattered, lying between 0.1 and 20, they all exceed 0.03. Therefore we conclude that the values of the thresholds have a negligible effect on the value of ϵ for Si.

To find the effect of plasmon intervention in the cascade of scattering events, Eqs. (24) and (25) were evaluated using values of $E_{th,n}$ and $\bar{E}_{th,n}$ from Eqs. (22) and (23). This yields four values for the pair-creation energy: $\epsilon_k(\hbar\omega_p)$, $\epsilon_{\bar{k}}(\hbar\omega_p)$, $\bar{\epsilon}_k(\hbar\omega_p)$, and $\bar{\epsilon}_{\bar{k}}(\hbar\omega_p)$, where $\hbar\omega_p$ is given in Table I. As functions of $\hbar\omega_p$, the first two of these for $A = 0$ in Si are plotted in Fig. 4; $\epsilon(E)$ for $A = 0$ from Fig. 2 is also shown. For $A = 0$, there is no phonon scattering for $E \geq E_{th}$; so $\hbar\omega_0$ is no longer a parameter of the calculations. Then ϵ, E, and $\hbar\omega_p$ can be scaled in units of E_g; Fig. 4 shows these functions thus scaled. The functions $\bar{\epsilon}(E)$, $\bar{\epsilon}_{\bar{k}}(\hbar\omega_p)$, and

TABLE I. The measured band gaps,[a] E_g, long-wavelength optical-phonon energies, $\hbar\omega_0$, and pair-creaction energies, ϵ, are tabulated below together with the plasmon energies, $\hbar\omega_p$, calculated from the lattice parameter.[b] All quantities are given in units of eV.

Semiconductor	E_g	$\hbar\omega_0$	Reference	$\hbar\omega_p$	ϵ	Reference
InSb	0.17	0.023	d	12.7		
PbS	0.41	0.026	e	14.5		
Ge	0.735	0.037	f	15.6	2.96	u
Si	1.12	0.063	g	16.6	3.63	v
GaAs	1.42	0.034	d	15.6	4.35	w
CdTe	1.52	0.021	h	12.8	4.46	x
HgI_2	2.13	0.007	i	13.7	4.2	y
GaP	2.22	0.045	j	16.5	6.54	z
CdS	2.41	0.038	k	15.0	6.3	a′
AgBr	2.68	0.016	l	15.2	5.8	b′
PbO	2.76	0.054	m	16.7	8	c′
SiC	2.86	0.120	n	23.2	6.9	d′
AgCl	3.25	0.024	o	16.0	7.5	e′
ZnO	3.35	0.073	p	21.5		
ZnS	3.87	0.043	q	16.7		
CaS	4.8	0.047	r	15.4		
C	5.47	0.163	s	31.0	13.1	f′
SiO_2	8.9[c]	0.081	t	24.2	18	g′

[a] Unless otherwise indicated, the band gaps are from W. H. Strehlow and E. L. Cook, J. Phys. Chem. Ref. Data 2, 163 (1973).

[b] R. W. G. Wyckoff, *Crystal Structures*, 2nd ed. (Wiley Interscience, New York, 1963), Vol. 1; see also Ref. 2.

[c] D. L. Griscom, J. Non-Cryst. Solids 24, 155 (1977).

[d] M. Hass and B. W. Henvis, J. Phys. Chem. Solids 23, 1099 (1962).

[e] R. Geick, Phys. Lett. 10, 51 (1964).

[f] B. N. Brockhouse and P. K. Iyengar, Phys. Rev. 111, 747 (1958).

[g] H. Palevsky, D. J. Hughes, W. Kley, and E. Tunkelo, Phys. Rev. Lett. 2, 258 (1959).

[h] M. Selders, E. Yi Chen, and R. K. Chang, Solid State Commun. 12, 1057 (1973).

[i] T. Goto and Y. Nishina, Solid State Commun. 25, 123 (1978). The average energy of the three longitudinal-optical-phonon energies of 0.0024, 0.004, and 0.0145 eV was taken.

[j] J. L. Yarnell, J. L. Warren, R. G. Wenzel, and P. J. Dean, in *Neutron Inelastic Scattering*, (IAEA, Vienna, 1968), Vol. 1, p. 301.

[k] R. J. Collins, J. Appl. Phys. 30, 1135 (1959).

[l] W. von der Osten and B. Dorner, Solid State Commun. 16, 431 (1975).

[m] D. M. Adams and D. C. Stevens, J. Chem. Soc. 1096 (1977).

[n] J. F. Vetelino and S. S. Mitra, Phys. Rev. 178, 1349 (1969).

[o] P. R. Vijayaraghavan, R. M. Nicklow, H. G. Smith, and M. K. Wilkinson, Phys. Rev. B 1, 4819 (1970).

[p] R. J. Collins and D. A. Kleinman, J. Phys. Chem. Solids 11, 190 (1959).

[q] N. Vagelatos, D. Wehe, and J. S. King, J. Chem. Phys. 60, 3613 (1974).

[r] M. Drofenik and A. Azman, J. Phys. Chem. Solids 33, 761 (1971).

[s] *The Properties of Diamond*, edited by J. E. Field (Academic, New York, 1979).

[t] J. F. Scott and S. P. S. Porto, Phys. Rev. 161, 903 (1967). The average of the eight longitudinal-optical-phonon energies was taken.

[u] R. H. Pehl, F. S. Goulding, D. A. Landis, and M. Lenglinger, Nucl. Instrum. Methods 59, 45 (1968).

[v] Reference 38.

[w] T. Kobayashi, T. Sugita, M. Koyama, and S. Takayanagi, IEEE Trans. Nucl. Sci. NS-19, 324 (1972).

[x] A. Cornet, P. Siffert, A. Coche, and R. Triboulet, Appl. Phys. Lett. 17, 432 (1970).

[y] J. P. Ponpon, R. Stuck, P. Siffert, B. Meyer, and C. Schwab, IEEE Trans. Nucl. Sci. NS-22, 182 (1975); see also M. Slapa, G. C. Huth, W. Seibt, M. M. Schieber, and P. T. Randtke, *ibid.* NS-23, 102 (1976).

[z] T. Kobayashi, Appl. Phys. Lett. 21, 150 (1972).

[a′] P. Eichinger and H. Kallmann, Appl. Phys. Lett. 25, 676 (1974).

[b′] K. A. Yamakawa, Phys. Rev. 82, 522 (1951).

[c′] Reference 8.

TABLE I (*Continued*)

[d] V. V. Makarov, Fiz. Tekh. Poluprovodn. 9, 798 (1975); 9, 1098 (1975) [Sov. Phys.—Semicond. 9, 526 (1975); 9, 722 (1975)].

[e] F. C. Brown, Phys. Rev. 97, 355 (1955).

[f] S. F. Kozlov, R. Stuck, M. Hage-Ali, and P. Siffert, IEEE Trans. Nucl. Sci. NS-22, 160 (1975).

[g] Reference 30.

$\bar{\epsilon}_{\bar{k}}(\hbar\omega_p)$ for $A = 0$ have a form similar to the functions shown in Fig. 4. For $A = 5.2$ eV^3, $\epsilon(E)$, $\epsilon_k(\hbar\omega_p)$, and $\epsilon_{\bar{k}}(\hbar\omega_p)$ are shown in Fig. 5; $\bar{\epsilon}(E)$, $\bar{\epsilon}_k(\hbar\omega_p)$, and $\bar{\epsilon}_{\bar{k}}(\hbar\omega_p)$ for this A are indistinguishable from these functions. All three functions shown in Fig. 4 closely approach a common value at energies even below $15E_g$, the value of $\hbar\omega_p$ for Si. Likewise, all three functions shown in Fig. 5 closely approach a common value at energies even below $\hbar\omega_p = 16.6$ eV for Si. Therefore we conclude that plasmon intervention has a insignificant effect on the value of ϵ for Si.

The functions $p_n(E)$ for $0 \leq n \leq 7$ and $0 \leq E \leq 15$ eV are shown in Figs. 6 and 7 for $A = 0$ and 5.2 eV^3, respectively. These functions in Figs. 6 and 7 were used in the calculations of the ϵ curves of Figs. 2–5. The $p_n(E)$ distributions used for ϵ and $\bar{\epsilon}$ are different for $A = 0$ but are indistinguishable for $A = 5.2$ eV^3.

The maxima of the $p_n(E)$ in Fig. 7 lie at larger energies than those of Fig. 6. These increases are due to competition with phonon generation above the threshold energies $E_{\text{th},n}$. These $p_n(E)$ functions for $A = 5.2$ eV^3 have non-negligible values only at energies substantially above the $E_{\text{th},n}$. Thus the precise values of $E_{\text{th},n}$ are unimportant, and $p_n(E)$ for $E_{\text{th},n}$ and $\bar{E}_{\text{th},n}$ are indistinguishable.

The values of $\epsilon(E)$ and $\bar{\epsilon}(E)$ shown in Fig. 2 do approach a constant value at large E, but they do so only at E large compared to $10E_g$, an energy region for which the calculations become prohibitively[36] expensive. Thus we cannot obtain ϵ by examining its asymptotic behavior. We do, however, know that $\epsilon = \epsilon_k(\infty) = \epsilon_{\bar{k}}(\infty)$ and $\bar{\epsilon} = \bar{\epsilon}_k(\infty) = \bar{\epsilon}_{\bar{k}}(\infty)$, and that the quantum-yield curves are closely linear for energies above a few times the band gap. In Figs. 4 and 5, $\epsilon_{\bar{k}}(\hbar\omega_p)$ appears to approach a constant value at lower energies than do $\epsilon(E)$ and $\epsilon_k(\hbar\omega_p)$; the overscored functions behave the same way. Therefore we have adopted the operational definitions $\epsilon = \epsilon_{\bar{k}}(7E_g)$ and $\bar{\epsilon} = \bar{\epsilon}_{\bar{k}}(6E_g)$.

These choices reflect limitations imposed by cost considerations. They allow obtaining ϵ and $\bar{\epsilon}$ with the n index in Eq. (1) restricted to $0 \leq n \leq 4$. The energies $7E_g$ for ϵ and $6E_g$ for $\bar{\epsilon}$ are the largest energies for which $p_5(E)$ is insignificant, because $E_{\text{th},5} = 5.67E_g$ from Eq. (22) and $\bar{E}_{\text{th},5} = 5E_g$ from Eq. (23). With some expense, we have extended[37] the Si calculations to $0 \leq n \leq 7$, as shown in Figs. 2–7, and ϵ changed by less than 1%.

Since there have been many[38,39] measurements of

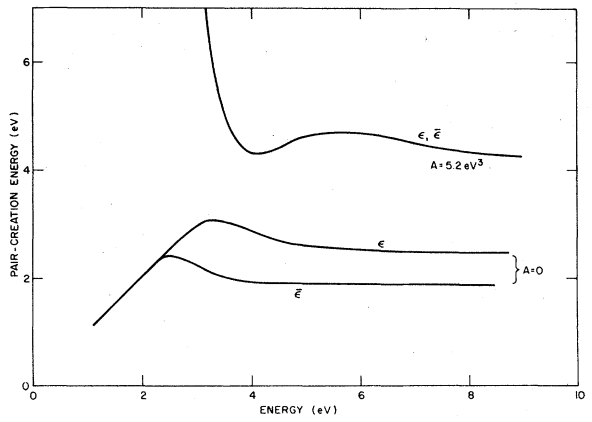

FIG. 2. Pair-creation energies for particles of energy E are plotted for the band gap and phonon energy of Si. These energies, calculated with E_{th} and $\bar{E}_{\text{th}}$, namely $\epsilon(E)$ and $\bar{\epsilon}(E)$, respectively, are shown both for no phonon scattering above the ionization threshold energy ($A = 0$), and also for a selected amount of phonon scattering ($A = 5.2$ eV^3). In this latter case the two curves are identical. The calculation of $\epsilon(E)$ extends to larger energies than that of $\bar{\epsilon}(E)$ because the $E_{\text{th},n}$ exceed the $\bar{E}_{\text{th},n}$.

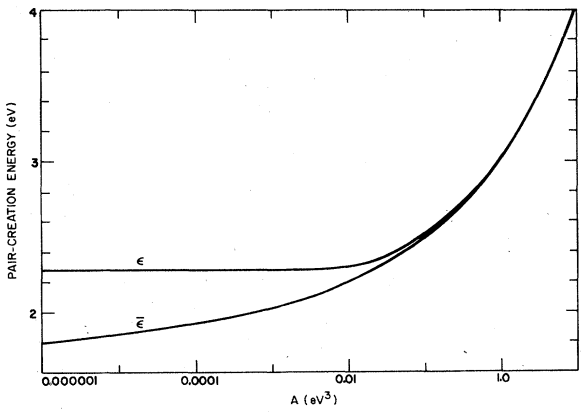

FIG. 3. Pair-creation energies ϵ and $\bar{\epsilon}$ are plotted versus the parameter A, which describes the relative amounts of scattering by phonon emission and by ionization. These values of ϵ and $\bar{\epsilon}$ were calculated for the band gap and phonon energy of Si.

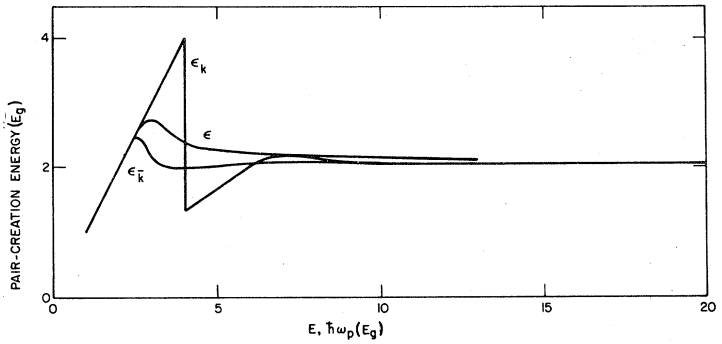

FIG. 4. Pair-creation energies $\epsilon(E)$, $\epsilon_k(\hbar\omega_p)$, and $\epsilon_{\bar{k}}(\hbar\omega_p)$ are plotted versus E and $\hbar\omega_p$. These functions describe pair creation by a particle of energy E and by a plasmon of energy $\hbar\omega_p$; momentum conservation and nonconservation in the plasmon decay are indicated by the subscripts k and $\bar{k}$. The values were calculated with Eq. (22) and with $A = 0$. Since phonon scattering above the ionization threshold is ignored, energies are scaled in units of E_g and these curves apply to all semiconductors.

the pair-creation energy in Si, all of which yield values close to 3.63 eV, this value was used with Fig. 3 to assign the value 5.2 eV^3 to A for all subsequent calculations. Using this value of A and the values of E_g, $\hbar\omega_0$, and $\hbar\omega_p$ given in Table I, the pair-creation energies shown in Table II were calculated for many semiconductors. These are in good accord with the measured pair-creation energies shown in Table I, as illustrated in Fig. 8.

The insensitivity of ϵ to the threshold energy and to plasmon intervention found in Si extends to many many, but not all, other semiconductors shown in Table II. For example, for SiO_2, ϵ and $\bar{\epsilon}$ differ considerably. The source of this difference is its large band gap; a large band gap reduces the ratio $r'(E)/r(E)$. For a large enough band gap, when $E_{th} > E_g$, this ratio, as shown in Eq. (20), will be less than unity for all $E > E_{th}$. Then values of ϵ and of $\bar{\epsilon}$ calculated with $A = 5.2$ eV^3 will differ little from their values calculated with $A = 0$. As seen in Fig. 2, however, when $A = 0$, ϵ and $\bar{\epsilon}$ differ considerably. As another example, also for SiO_2, where $\hbar\omega_p/E_g$ is small, $\epsilon_k(\hbar\omega_p)$ and $\epsilon_{\bar{k}}(\hbar\omega_p)$ differ from the constant values approached by these functions at large $\hbar\omega_p$, and so these pair-creation energies differ from ϵ. These differences will be reduced when $\epsilon_k(\hbar\omega_p)$ and $\epsilon_{\bar{k}}(\hbar\omega_p)$ are averaged over the width of the plasmon resonance. In particular, the discontinuity in $\epsilon_k(\hbar\omega_p)$ shown in Fig. 4 for $\hbar\omega_p$ near $4E_g$ would be softened by this averaging.

In any event, these differences among the pair-creation energies shown in Table II are insufficient to establish the importance of either the threshold energy or plasmon intervention; for example, a plot of the measured pair-creation energies versus $\bar{\epsilon}_{\bar{k}}(\hbar\omega_p)$ shows agreement equal to that shown in Fig. 8.

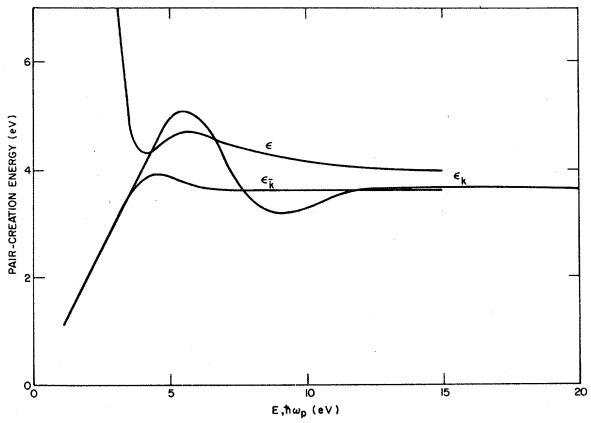

FIG. 5. Pair-creation energies $\epsilon(E)$, $\epsilon_k(\hbar\omega_p)$, and $\epsilon_{\bar{k}}(\hbar\omega_p)$ are plotted versus E and $\hbar\omega_p$ as in Fig. 4. These values were calculated for $A = 5.2$ eV^3 for the bandgap and phonon energy of Si. The values are indistinguishable from those of $\bar{\epsilon}(E)$, $\bar{\epsilon}_k(\hbar\omega_p)$, and $\bar{\epsilon}_{\bar{k}}(\hbar\omega_p)$ for this value of A.

B. Quantum yield

As was mentioned in the Introduction, the quantum yield is the average number of pairs created

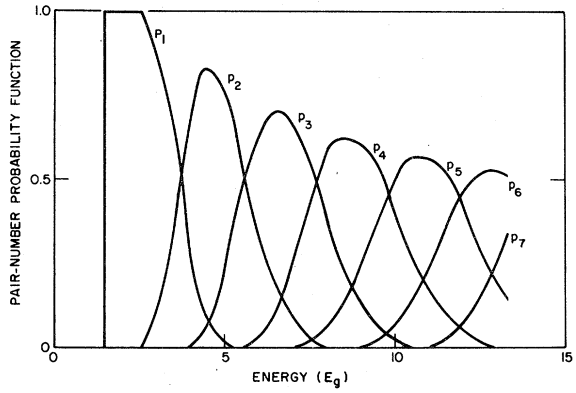

FIG. 6. Functions $p_n(E)$ for $1 \leq n \leq 7$ are plotted versus energy E. These functions were calculated with Eq. (22) and with $A = 0$; thus, as in Fig. 4, they are universal for all band gaps E_g.

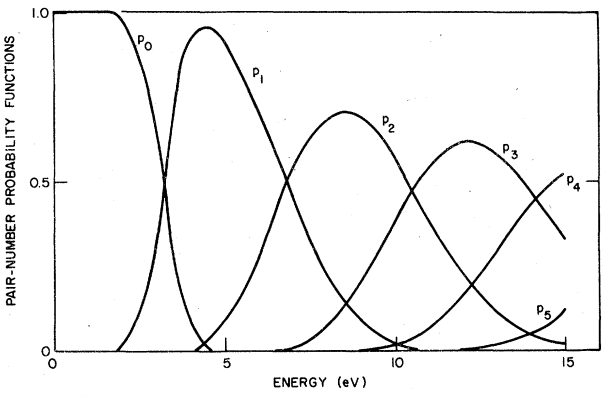

FIG. 7. Functions $p_n(E)$ for $0 \leq n \leq 5$ are plotted versus energy E. These functions were calculated for $A = 5.2$ eV^3 for the band gap and phonon energy of Si. Functions calculated with Eq. (22) and with Eq. (23) were indistinguishable at all energies.

by a particle entering a semiconductor; the quantum yield will be a function of the particle energy in the semiconductor. The particles for which quantum-yield measurements have been made include electrons and photons. For electrons the quantum yield is $\langle n(E) \rangle$ from Eq. (1), where E is the particle kinetic energy in the semiconductor. For flat bands, unaffected by injected charge, this energy is the kinetic energy in vacuum plus the electron affinity of the semiconductor. Measurements of $\langle n(E) \rangle$ have been reported only for CdS (Ref. 40) and ZnO (Ref. 41). These are compared with values calculated with $A = 5.2$ eV^3 in Figs. 9(a) and 9(b).

Since photons decay with momentum conservation from a state near $k = 0$, the quantum yield from photons is

$$\eta(h\nu) = h\nu/\epsilon_k(h\nu)\,, \tag{33}$$

where $h\nu$ is the photon energy and $\epsilon_k(h\nu)$ is identical to $\epsilon_k(\hbar\omega_p)$ defined in Eq. (24) with $\hbar\omega_p$ replaced by $h\nu$. Measurements of $\eta(h\nu)$ have been made in Si,[42-44] Ge,[42,43] PbS,[45,46] and InSb.[47] Measured values of $\eta(h\nu)$ for these materials and values calculated with $A = 5.2$ eV^3 are shown in Figs. 10 and 11.

C. Temperature dependence

In the model described in the previous sections, a temperature dependence for ϵ arises only from temperature dependences of E_g and $\hbar\omega_0$, i.e.,

$$\Delta\epsilon(T) = \frac{\partial\epsilon}{\partial E_g}\,\Delta E_g(T) + \frac{\partial\epsilon}{\partial\hbar\omega_0}\,\Delta\hbar\omega_0(T)\,. \tag{34}$$

For the semiconductors listed in Table I, the temperature dependence of $\hbar\omega_0$ is very weak so $\Delta\hbar\omega_0(T)$ was set to zero. By calculating the $\Delta\epsilon$ associated with a ΔE_g, values of $\partial\epsilon/\partial E_g$ were obtained.

Recent measurements of $\partial\epsilon/\partial E_g$ have been made in Si (Refs. 38 and 48); the measured values extend from 1.8 to 2.9 and are larger than the value calculated[49] here of 1.6. There is considerable scatter in the measured $\partial\epsilon/\partial E_g$ values in Si and other materials.[48] Thus any meaningful comparison of these calculations with experiment is not possible at present.

D. Fano factor

The Fano factor, being a measure of $\langle n^2 \rangle$, provides additional information about the $p_n(E)$ distri-

TABLE II. Calculated values of the pair-creation energy ϵ and Fano factor F are tabulated below. Six values of ϵ, in units of eV, were calculated, i.e., values of ϵ, $\epsilon_{\bar{k}}(\hbar\omega_p)$, and $\epsilon_k(\hbar\omega_p)$ calculated with Eq. (22), and $\bar{\epsilon}$, $\bar{\epsilon}_{\bar{k}}(\hbar\omega_p)$, and $\bar{\epsilon}_k(\hbar\omega_p)$ calculated with Eq. (23). Of the six values of the Fano factor, only F is listed.

Semiconductor	ϵ	$\epsilon_{\bar{k}}(\hbar\omega_p)$	$\epsilon_k(\hbar\omega_p)$	$\bar{\epsilon}$	$\bar{\epsilon}_{\bar{k}}(\hbar\omega_p)$	$\bar{\epsilon}_k(\hbar\omega_p)$	F
Ge	2.78	2.78	2.78	2.78	2.78	2.78	0.13
Si	3.63	3.63	3.67	3.63	3.63	3.67	0.115
GaAs	3.90	3.90	3.99	3.87	3.87	3.98	0.10
CdTe	3.90	3.91	3.98	3.87	3.87	3.97	0.10
HgI_2	4.65	4.64	4.55	4.58	4.58	4.53	0.08
GaP	5.37	5.37	5.36	5.33	5.33	5.34	0.09
CdS	5.63	5.62	5.02	5.59	5.59	5.00	0.09
AgBr	5.82	5.80	5.07	5.73	5.73	5.07	0.08
PbO	6.36	6.35	5.63	6.31	6.31	5.57	0.09
SiC	6.88	6.89	7.11	6.84	6.84	7.08	0.09
AgCl	6.94	6.87	5.35	6.81	6.75	5.32	0.08
ZnO	7.50	7.49	7.18	7.42	7.43	7.14	0.09
ZnS	8.23	8.03	5.57	8.06	7.88	5.57	0.08
CaS	10.0	10.1	15.4	9.6	9.5	5.13	0.08
C	11.6	11.6	10.4	11.3	11.3	10.3	0.08
SiO_2	18.3	21.0	24.2	16.6	17.3	24.2	0.08

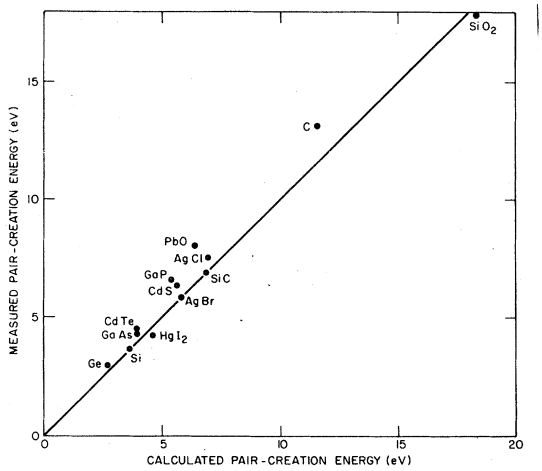

FIG. 8. Measured values of the pair-creation energy, listed in Table I, are plotted versus the calculated values of ϵ listed in Table II. The straight line has unit slope and is the locus of perfect agreement.

bution. The procedures used in the calculation of the pair-creation energy were repeated in the calculation of the Fano factor. We have evaluated the Fano factor both for E_{th} and $\overline{E}_{th}$ in the scattering by ionization. The values of F and $\overline{F}$ calculated for Si

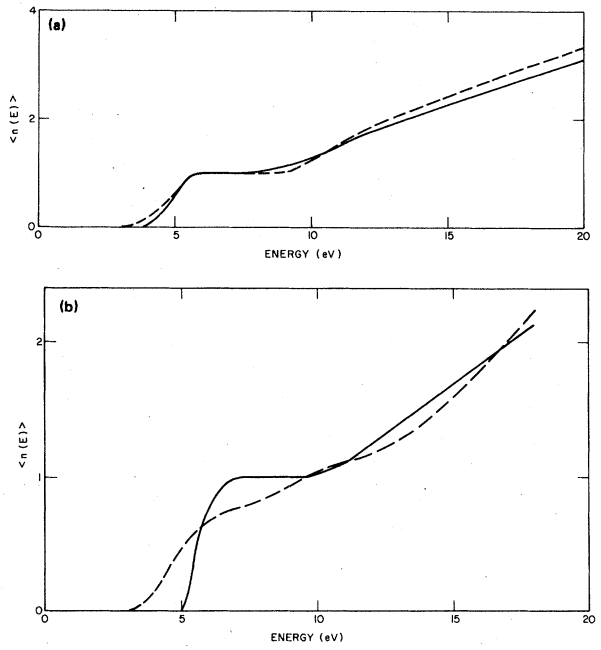

FIG. 9. Quantum-yield curves for electron excitation, $\langle n(E)\rangle$, are plotted versus electron energy E in (a) and (b) for CdS and ZnO. The calculated curves are shown by solid lines and the measurements by dashed lines. The measurements, given in Ref. 40 for CdS and in Ref. 41 for ZnO, are presented in arbitrary units. The calculations for CdS were done with $E_g = 2.57$ eV, the band gap at the measurement temperature, 80 K.

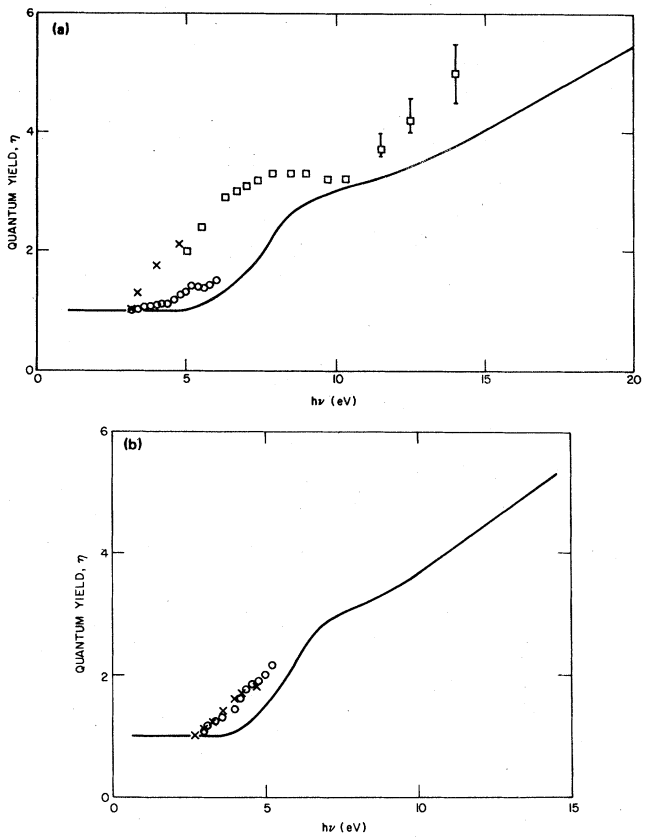

FIG. 10. Quantum-yield curves for photon excitation $\eta(h\nu)$ are plotted versus photon energy $h\nu$ in (a) and (b) for Si and Ge. The calculated curves are shown by solid lines. The measurements marked (×) were taken from Ref. 43; those marked (○) from Ref. 42, and those marked (□) from Ref. 44.

are plotted as a function of A in Fig. 12. These curves are analogous to the curves of ϵ and $\overline{\epsilon}$ in Fig. 3. Unlike those values, the values of F and $\overline{F}$ coincide for all A, as expected from the two-level approximation.

By analogy to Eqs. (24) and (25) for $\epsilon_k(\hbar\omega_p)$ and $\epsilon_{\overline{k}}(\hbar\omega_p)$, equations for the Fano factors $F_k(\hbar\omega_p)$ and $F_{\overline{k}}(\hbar\omega_p)$ can be written for the assumption of energy deposition into the plasmons and plasmon decay with and without momentum conservation. Plots of the functions $F(E)$, $F_k(\hbar\omega_p)$, and $F_{\overline{k}}(\hbar\omega_p)$ are shown in Fig. 13 for $A = 0$, analogous to the plots of the pair-creation energy in Fig. 4. Also plots of these functions are shown in Fig. 14 for $A = 5.2$ eV^3, analogous to the plots of the pair-creation energy in Fig. 5. The $F(E)$, $F_k(\hbar\omega_p)$, and $F_{\overline{k}}(\hbar\omega_p)$ converge toward a common value as E and $\hbar\omega_p$ increase. Figures 13 and 14 were calculated using $E_{th,n}$ of Eq. (22). The functions $\overline{F}(E)$, $\overline{F}_k(\hbar\omega_p)$, and $\overline{F}_{\overline{k}}(\hbar\omega_p)$ using $\overline{E}_{th,n}$ of Eq. (23) are very similar to $F(E)$, $F_k(\hbar\omega_p)$, and $F_{\overline{k}}(\hbar\omega_p)$, respectively, for both $A = 5.2$ eV^3 and 0.

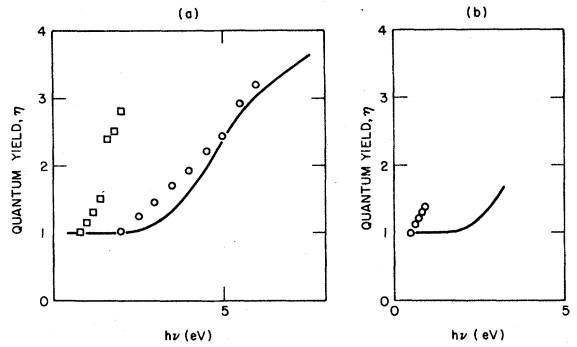

FIG. 11. Quantum-yield curves $\eta(h\nu)$, as in Fig. 10, are shown in (a) and (b) for PbS and InSb. For PbS the measurements marked by (○) were taken from Ref. 45, and those marked by (□) from Ref. 46. For InSb the measurements marked by (○) were taken from Ref. 47.

The measured[50] Fano factors in Si and Ge are near 0.1 and 0.13, respectively; the calculated values of 0.115 and 0.13 shown in Table II are in good accord with these measurements. Although six values of the Fano factor were calculated, analogous to the six values of the pair-creation energy shown in Table II, the differences among these six values were much less than the uncertainties in the experimental data, so only the value of F was included in Table II.

IV. DISCUSSION

A. Precedents

Several calculations of the pair-creation energy in the literature were repeated during the course of this work. These calculations will be described here. Van Roosbroeck,[10] using the assumption that only energy is conserved in the scattering processes, calculated E_K, the average energy loss to the lattice by a final particle; he found, for no phonon losses above threshold, this loss E_K to be $0.285E_g$; hence, $\epsilon = 2E_K + E_g = 1.57E_g$. This calculation was done under the same conditions as our calculation of $\bar{\epsilon}$ for $A = 0$; as shown in Fig. 3, $\bar{\epsilon} = 1.62E_g$ for $A = 0$.

Drummond and Moll[12] used $\bar{E}_{th}$ and they departed from the free-particle approximation by using Kane's $r(E)$ and $r'(E)$ which Kane calculated using his electron-band structure and phonon dispersion for Si. With two different values of the ratios of the rates of scattering by phonon emission and ionization, i.e., of ratios analogous to A, they calculated values of 4.02 and 3.53 eV for $\bar{\epsilon}$, excluding their phonon contributions, $\langle E_R \rangle$. When these departures from the free-particle approximation were incorporated into our calculation of $p_0(E)$ for these two ratios, their published curves for $PI(E) \equiv 1 - p_0(E)$ were reproduced. These functions $p_0(E)$ were used[51] to obtain $p_n(E)$ from which values of 4.07 and 3.59 eV for $\bar{\epsilon}$ were calculated.

Rothwarf[1] developed a set of thresholds for the creation of multiple pairs in the decay of a plasmon, assuming the energy of the incident particle is deposited into plasmons. He assumes that the plasmons decay with momentum conservation and he used E_{th} as given by Eq. (22). He neglects phonon scattering above the threshold energy. His calculation was done under the same conditions as our calculation of $\epsilon_k(\hbar\omega_p)$ for $A = 0$ shown in Fig. 4. He finds $\epsilon_k(\hbar\omega_p)$ should have unit slope for $1 \leq \hbar\omega_p/E_g \leq 4$ and slope $\frac{1}{3}$ for $4 \leq \hbar\omega_p/E_g \leq 12$. For $\hbar\omega_p \lesssim 6E_g$ these features are clearly evident in the plot of $\epsilon_k(\hbar\omega_p)$ shown in Fig. 4; for $\hbar\omega_p > 6E_g$ particles created by the plasmon scatter to several states and $\epsilon_k(\hbar\omega_p)$ approaches ϵ.

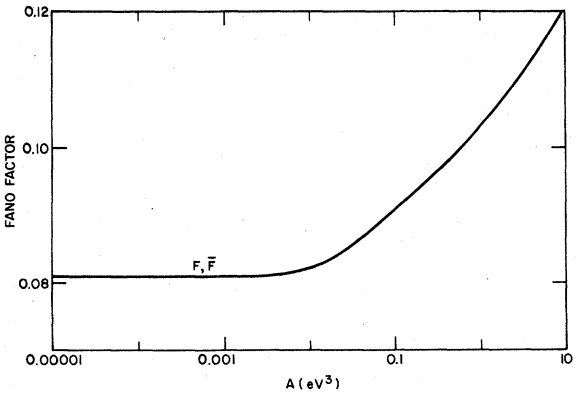

FIG. 12. Fano factors F and $\bar{F}$ are plotted versus A for silicon; this figure is the analog of Fig. 3.

B. Ion-pair creation energy

The calculation of the pair-creation energy in semiconductors uses many concepts which also appear in the calculation of the mean energy W expended in producing an ion pair in a gas by an energetic charged particle.[52] For example, the direct calculation of the number of ion pairs from the excitation cross sections[53,54] closely resembles the calculation of the number of final particles using the final-state method, Eq. (28). The calculations differ in that only two, instead of three, energetic charged particles result from the creation of an ion pair; the ion corresponds to a very heavy hole. Also, whereas a semiconductor may be treated as having only one nonionizing scattering mechanism, viz., the creation of monoenergetic phonons, a molecule must be treated as having a number of nonionizing excitations. In another example, the moments of

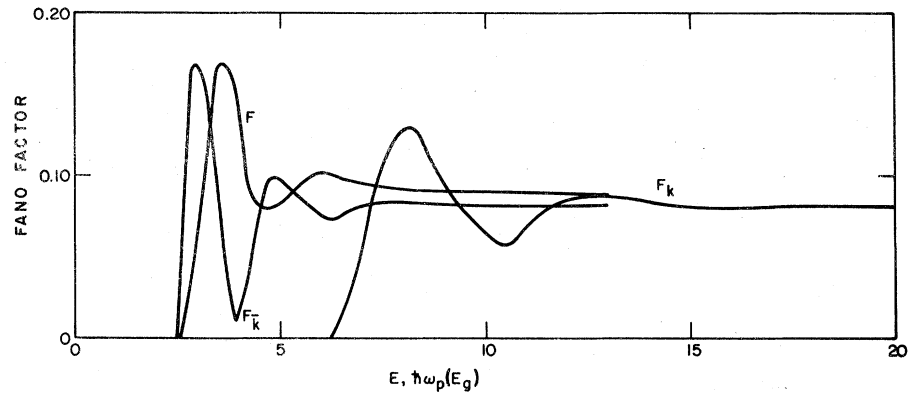

FIG. 13. Fano factors $F(E)$, $F_k(\hbar\omega_p)$, and $F_{\bar{k}}(\hbar\omega_p)$ are plotted versus E and $\hbar\omega_p$ for $A=0$; this figure is the analog of Fig. 4.

the probabilities that a particle of energy E creates n ion pairs, analogous to the $p_n(E)$ used here, have been related[55] to the Spencer-Fano degradation spectrum, used[52] in the calculation of W.

C. Scattering-rate ratio

The parameter A, defined in Eq. (21), is proportional to the ratio of the matrix elements for electron scattering by phonon emission and by ionization. It seems inexplicable that A is independent of particle energy, i.e., that $(|M'|/|M|)^2$ in Eq. (21) is a constant independent of the initial particle energy, although this is known from the work of Kane. It is surprising that Eq. (20), obtained from the free-particle model, with A a constant, should describe the energy dependence of the ratio of the scattering rates, as illustrated by the quantum-yield data. It is astonishing that the experimental data in a dozen different semiconductors can be described so well with a single value of this parameter. The success of Eq. (20) implies a lack of dependence on the details of electron-band structure. The value of A is an empirical result of the work described here and we do not attempt to account for it.

Although we shall not account for this value of A, a dimensional analysis of A is interesting. Using

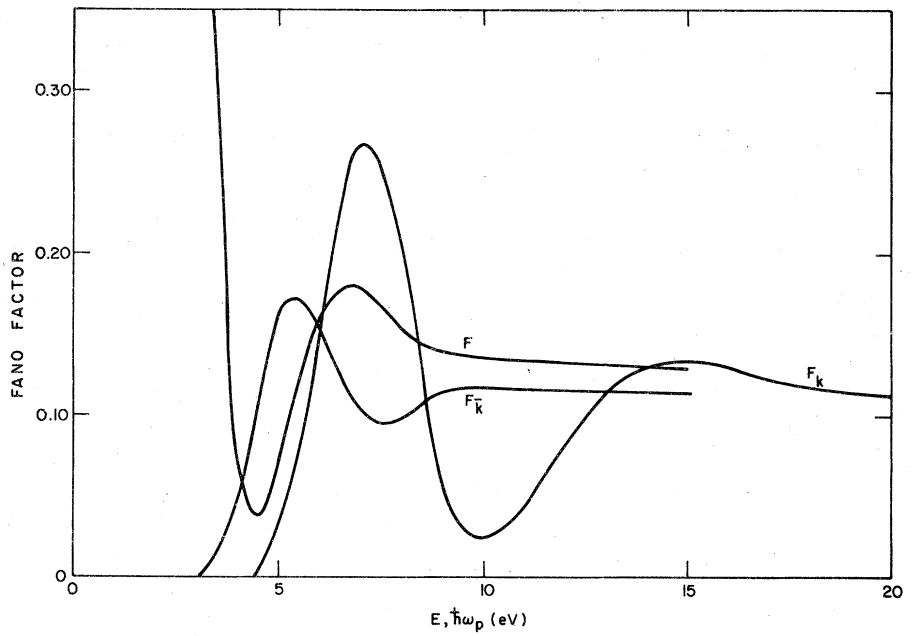

FIG. 14. Fano factors $F(E)$, $F_k(\hbar\omega_p)$, and $F_{\bar{k}}(\hbar\omega_p)$ are plotted versus E and $\hbar\omega_p$ for $A=5.2$ eV^3 in Si; this is the analog of Fig. 5.

the Bohr radius, $a_0 = \hbar^2/me^2$, Eq. (21) becomes

$$A = \frac{\pi^4}{2}\left(\frac{|M'|}{|M|}\right)^2 \frac{e^6 a_0^3}{V\Delta} . \tag{36}$$

From the electron-phonon interaction,[56] $|M'|^2$ is approximately $\pi e^2 \hbar\omega_0/2Vq^2$, where $\hbar q$ is the momentum transfer in the scattering process. From the Coulomb interaction,[17] M is approximately $4\pi e^2/q^2V$. Therefore A is of order $(\hbar\omega_0)(e^2q)^2(a_0^3/\Delta)$. Taking q to be a reciprocal screening length of the valence band, q is of order $2/a_0$. Then for $\hbar\omega_0 \sim 0.05$ eV and $\Delta \sim 100\ a_0^3$, A is of order 1 eV^3. Thus the value found empirically, 5.2 eV^3, is of the expected order of magnitude. This estimate contains only the contribution from the interaction with the polar optical phonons; there is also a contribution from the optical-mode deformation potential.[57] This latter contribution may in fact be dominant since a single value of A describes both polar and nonpolar semiconductors.

The ratio of the mean free paths for scattering by ionization and by phonon emission is related to the scattering rates by[16]

$$\frac{l_i}{l_p} = \frac{r'(E)}{r(E)} \approx \frac{(105A/2\pi)E^{1/2}}{(E-E_g)^{7/2}} \tag{37}$$

from Eq. (20). Measurements of these mean free paths have been made[35] by avalanche breakdown, electron emission, nonavalanche injection, etc., and theoretical calculations[58] have also been published. The values of l_i and l_p generally lie around 100 Å for kinetic energies near 5 eV in Si. For $A = 5.2$ eV^3, Eq. (37) yields $l_i/l_p = 1.7$ for $E = 5$ eV in Si, in good accord with the published data.

Although scattering by ionization is possible for all energies above the threshold energy, the mean free path for ionization may greatly exceed that for phonon emission at some of these energies, as seen from Eq. (37). The energy E_q at which these two mean free paths are equal depends on the band gap. Thus for $E_g \approx 0$ eV, $E_q \approx 4.4$ eV while for $E_g = 10$ eV, $E_q = 1.5E_g$, assuming $A = 5.2$ eV^3 in Eq. (37). Therefore, the value of $h\nu$ at which $\eta(h\nu)$ in Eq. (33) rises from 1 to 3 may greatly exceed $4E_g$. This behavior is exhibited in Figs. 10 and 11, and it is particularly evident for InSb, where $\eta < 1.5$ was calculated for $E < 17E_g$.

In calculating the upper theoretical limit of efficiency of p-n junction solar cells, Shockley and Queisser[59] note that this limit is restricted to unit quantum yield for solar photons. As they observe, the quantum yields of Si, Ge, and other materials, shown in Figs. 10 and 11, do not appreciably exceed unity for $h\nu \lesssim 3$ eV, the upper bound on the terrestrial solar photon energy. One might at first expect that by going to small-band-gap materials the quantum yield would rise above unity within the range of available solar photons, and this would thus enhance the solar-cell efficiency at low temperatures. Such is true, however, only for very small A values. As was discussed in a previous paragraph, the usual values of A imply strong phonon competition and give the energies for higher-than-unity quantum yields well above the upper cutoff of the solar spectrum. A similar conclusion has been reached[60] through the use of Shockley's[9] approximation to the quantum-yield curve.

D. General formulas for ϵ

As was noted in the Introduction, the assumption[9] of uniform population has acquired some degree of popular support because it yields a general formula for $\epsilon(E_g)$, viz., $\epsilon = A'E_g + B'$, which is in good accord with the measured correlation between ϵ and E_g in many semiconductors. In addition the value of A' estimated kinematically is close to that found empirically.[14] In contrast, up to now a general formula for computing ϵ has not been given using the scattering-rate assumption. In this paper this scattering-rate assumption is used and the general formula for computing $\epsilon = \epsilon(A, E_g, \hbar\omega_0)$ is obtained, which is, adopting a single value of A, in good accord with the observed values of ϵ, E_g, and $\hbar\omega_0$ in many semiconductors, as shown in Fig. 8.

Except for HgI_2, the measured values of ϵ equal or exceed the calculated values shown in Fig. 8, neglecting the small difference for SiO_2. Although another value of A would yield better accord between these measured and calculated values, it would yield a poorer accord for Si, on which there is a wealth[38,39] of consistent measurements. Furthermore, the measured values of ϵ have generally decreased as new measurements, with presumably better collection efficiencies, are done. For example, the measured values of ϵ have changed from 7.8 to 6.54 eV (Ref. 61) for GaP, from 16 to 13.1 eV (Ref. 62) for diamond, from 9.0 to 6.9 eV (Ref. 63) for SiC, and from 7.2 to 6.3 eV (Ref. 64) for CdS; in contrast, there have been no measurements of ϵ which have resulted in a larger value. It is anticipated that future measurements of ϵ will be yet lower than those shown in Fig. 8. Therefore, at present the most reasonable value of A seems to be that fitted to ϵ for Si.

For HgI_2, the measured value of the pair-creation energy is inexplicable with $A = 5.2$ eV^3 within the theory presented here. It is indeed impossible that ϵ with any A will afford agreement. It is true that $\bar{\epsilon}$ for some $A < 5.2$ eV^3 will match the measured pair-creation energy in HgI_2, but values of $\bar{\epsilon}$ calculated with this A would be discordant with the measured values for all the other semiconductors.

E. Cathodoluminescence efficiency

The efficiency ξ of cathode-ray phosphors is[1,2,65] $\xi = SE_e/\epsilon$, where E_e is the energy of the emitted photon, ϵ is the pair-creation energy, and S is the efficiency of radiative recombination. Since $S \leq 1$, then $\epsilon \leq E_e/\xi$, and so measurements of E_e and ξ provide a measured upper bound on ϵ. For two of the most efficient phosphors, CaS:Ce and ZnS:Cu, the measured E_e is 2.3 eV for both and the measured ξ are 0.22 and 0.23, respectively; thus the measured upper bounds on ϵ are 10.5 and 10.0 eV in CaS and ZnS. For ZnS, as shown in Table II, the calculated pair-creation energies are all well below this upper bound. In fact, the calculated value of ϵ, 8.2 eV, yields $S = 0.82$ for $\xi = 0.23$, and it would imply $\xi = 0.28$ for $S = 1$. For CaS, as shown in Table II, except[66] for $\epsilon_k(\hbar\omega_p)$ and $\bar{\epsilon}_k(\hbar\omega_p)$, the calculated pair-creation energies are all near, but below, the measured upper bound, 10.5 eV. The calculated value of ϵ, 10.0 eV, yields $S = 0.95$ for $\xi = 0.22$. For other cathode-ray phosphors, the measured upper bounds on ϵ greatly exceed the calculated values, i.e., S is significantly less than unity.

V. CONCLUSIONS

The scattering-rate assumption is adopted, in preference to the assumption of uniform population, because it allows calculation of the population of the final states and is found to give nonuniform population of these states.

Using the scattering-rate assumption, we introduce a new probability method, and extend the earlier final-state method for solving the model equations. In the probability method, the pair-number probability distribution, $p_n(E)$, for the number n of pairs created by a primary particle of energy E is calculated. In the final-state method, the final-state distribution function, $L(E', E)$, is calculated. The $p_n(E)$ distribution is directly measurable and the pair-creation energy ϵ and Fano factor F are readily calculable from $\langle n \rangle$ and $\langle n^2 \rangle$. In contrast, the final-state distribution is not measurable and we cannot calculate the Fano factor using it.

We use the free-electron approximation in calculating these $p_n(E)$ distributions; and we obtain ϵ and F as parametric functions of the band gap E_g, the long-wavelength longitudinal-optical phonon energy $\hbar\omega_0$, and a parameter A proportional to the ratio of the mean free paths for scattering by ionization and by phonon emission. A single value of A, namely, that which makes the ϵ of Si agree with the experimental value, is found to give also good agreement for ϵ, F, and the quantum yield in many other semiconductors. Also, this value of A is consistent with existing measurements of the mean free paths. In addition, the calculated ϵ and F are found insensitive in many semiconductors to electron-energy loss to plasmons and to differences in the threshold energy for ionization representing real band-structure features.

---

[1] A. Rothwarf, J. Appl. Phys. 44, 752 (1973).
[2] R. C. Alig and S. Bloom, J. Electrochem. Soc. 124, 1136 (1977).
[3] K. G. McKay, Phys. Rev. 76, 1537 (1949).
[4] R. H. Pehl, Phys. Today 30 (11), 50 (1977); and F. S. Goulding, IEEE Trans. Nucl. Sci. NS-25, 916 (1978).
[5] R. C. Alig and S. Bloom, J. Appl. Phys. 49, 3476 (1978).
[6] A. J. Dekker, in *Solid State Physics*, edited by F. Seitz and D. Turnbull (Academic, New York, 1958), Vol. 6, p. 251.
[7] K. G. McKay and K. B. McAfee, Phys. Rev. 91, 1079 (1953).
[8] F. Lappe, J. Phys. Chem. Solids 20, 173 (1961).
[9] W. Shockley, Solid-State Electron. 2, 35 (1961).
[10] W. van Roosbroeck, Phys. Rev. 139, A1702 (1965).
[11] E. Antoncik, Czech. J. Phys. B 18, 157 (1968).
[12] W. E. Drummond and J. L. Moll, J. Appl. Phys. 42, 5556 (1971).
[13] C. A. Klein, J. Appl. Phys. 39, 2029 (1968).
[14] R. C. Alig and S. Bloom, Phys. Rev. Lett. 35, 1522 (1975).
[15] With momentum and energy conservation, the three particles resulting from scattering by ionization must have equal energies E' and collinear, equal momenta, if indeed E_{th} is the lowest energy for scattering by ionization. The magnitudes of these momenta are proportional to $\sqrt{E'}$ in the free-particle approximation. Thus $E_{th} = 3E' + E_g$ by energy conservation and $\sqrt{E_{th}} = 3\sqrt{E'}$ by momentum conservation, or $E_{th} = 3E_g/2$.
[16] E. O. Kane, J. Phys. Soc. Jpn. Suppl. 21, 37 (1966).
[17] E. O. Kane, Phys. Rev. 159, 624 (1967).
[18] A. Zareba, *Proceedings of the International Conference on Semiconductor Physics, Prague, 1960* (Academic, New York, 1961), p. 476.
[19] C. A. Klein, J. Phys. Soc. Jpn. Suppl. 21, 307 (1966); J. D. Kingsley and G. W. Ludwig, J. Electrochem. Soc. 117, 353 (1970).
[20] D. Pines, Rev. Mod. Phys. 28, 184 (1956).
[21] U. Fano, Phys. Rev. 72, 26 (1947).
[22] C. A. Klein, IEEE Trans. Nucl. Sci. NS-15, 214 (1968).
[23] T. Yamaya, R. Asano, H. Endo, and K. Umeda, Nucl. Instrum. Methods 159, 181 (1979).
[24] The expression for F derived in Ref. 22 using the final-state method yields $F = \frac{1}{6}$ in our two-level approximation; we cannot account for this discrepancy because we are unable to derive his expression from our Eq. (4).

[25]In Ref. 12, $P_m(E)$ is given as

$$P_m(E)=P_0(E-m\hbar\omega_0)\prod_{i=0}^{m-1}[1-P_i(E)].$$

This is incorrect because for very large E, $\sum_{m=0}^{\infty}P_m(E)$ must approach unity to conserve probability, and only our Eq. (9) fulfills this requirement. Since we were able to closely replicate the calculations given in Ref. 12, we suspect the form of $P_m(E)$ given there may be a misprint.

[26]J. F. Janak, A. R. Williams, and V. L. Moruzzi, Phys. Rev. B 11, 1522 (1975); N. Schwentner, *ibid.* 14, 5490 (1976).

[27]R. Klopfenstein, private communication.

[28]C. L. Anderson and C. R. Crowell, Phys. Rev. B 5, 2267 (1972); T. P. Pearsall, R. E. Nahory, and J. R. Chelikowsky, Phys. Rev. Lett. 39, 295 (1977).

[29]The derivation of $E_{\rm th}$ is given in Ref. 15. Equation (22) is derived in a similar manner, being the solution of

$$E_{{\rm th},n}=E_{{\rm th},n-1}+2E'+E_g,$$
$$\sqrt{E}_{{\rm th},n}=\sqrt{E}_{{\rm th},n-1}+2\sqrt{E'}\ .$$

[30]G. A. Ausman, Jr. and F. B. McLean, Appl. Phys. Lett. 26, 173 (1975).

[31]In the first step of Eq. (26), the number of pairs is the one created by the direct plasmon decay plus the average number created by the products of the direct plasmon decay. The second step of Eq. (26) follows from

$$\sum_{n=0}^{\infty}n\sum_{m=0}^{n}p_mp_{n-m}\equiv\sum_{i=0}^{\infty}\sum_{j=0}^{\infty}(i+j)\,p_ip_j=2\langle n\rangle\,.$$

[32]Drummond and Moll, Ref. 12, used this approach to calculate ϵ. They approximated Eq. (29) by

$$N(E',E)=PI(E)S(E',E-g(E)\hbar\omega_0)$$

and Eq. (30) by

$$S(E',E'')=3\int dE_e N(E',E_e)n(E'',E_e),$$

where $E''=E-g(E)\hbar\omega_0$ and $g(E)$, $PI(E)$, and $n(E'',E_e)$ are defined by Eqs. (3), (2), and (14) of Ref. 12. Instead of Eq. (31), they started with an ensemble of cascades originating on particles with energies distributed uniformly between 0 and 10 E_g. As a result, they obtained $d(E')\equiv\lim_{E\to\infty}L(E',E)$, instead of $N(E',E)$. They added a term $\langle E_R\rangle$ to their ϵ to account for phonon losses preceding ionization scattering events; thus ϵ was approximated by

$$\epsilon=2E_K+E_g+\langle E_R\rangle\,,$$

where

$$\langle E_R\rangle\equiv\hbar\omega_0\int_{E_1}^{E_2}g(E)dE(E_2-E_1)^{-1}\,,$$

and E_1 and E_2 were chosen to bound the peak of $g(E)$. This information was graciously provided by W. Drummond in a private communication.

[33]Requests for values of ϵ for desired values of E_g and $\hbar\omega_0$ will be honored.

[34]J. Shah, Solid-State Electron. 21, 43 (1978); D. von der Linde and R. Lambrich, Phys. Rev. Lett. 42, 1090 (1979).

[35]D. J. Bartelink, J. L. Moll, and N. I. Meyer, Phys. Rev. 130, 972 (1963); J. F. Verwey, R. P. Kramer, and B. J. de Maagt, J. Appl. Phys. 46, 2612 (1975); I. Shahriary, J. R. Schwank, and F. G. Allen, *ibid.* 50, 1428 (1979).

[36]The calculations of an ϵ used at times more than 400 cpu seconds of an IBM 370.

[37]It cannot be proved that $\epsilon_{\bar{k}}(7E_g)$ is identical with $\epsilon_{\bar{k}}(\infty)$. In fact, $\epsilon_{\bar{k}}(7E_g)$ may exceed $\epsilon_{\bar{k}}(\infty)$ because the particles created in the plasmon decay may have energies E such that $\epsilon(E)>\epsilon(\infty)$. On the other hand, $\epsilon_{\bar{k}}(\infty)$ may exceed $\epsilon_{\bar{k}}(7E)$ because the plasmon decay yields a pair with no phonon losses. However, in the extension of the calculations for Si, shown in Figs. 3 and 4, $\epsilon_{\bar{k}}(14E_g)$ and $\epsilon_{\bar{k}}(7E_g)$ differ by less than 1%.

[38]R. D. Ryan, IEEE Trans. Nucl. Sci. NS-20, 473 (1973).

[39]J. R. Fiebiger and R. S. Muller, J. Appl. Phys. 43, 3202 (1972); R. H. Pehl, F. S. Goulding, D. A. Landis, and M. Lenzlinger, Nucl. Instrum. Methods 59, 45 (1968).

[40]F. Steinrisser, Phys. Rev. Lett. 24, 213 (1970).

[41]R. E. Shrader and S. F. Kaisel, J. Opt. Soc. Am. 44, 135 (1954).

[42]O. Christensen, J. Appl. Phys. 47, 689 (1976).

[43]V. S. Vavilov, J. Phys. Chem. Solids 8, 223 (1959).

[44]A. J. Tuzzolino, Phys. Rev. 134, A205 (1964).

[45]A. Smith and D. Dutton, J. Opt. Soc. Am. 48, 1007 (1958).

[46]V. N. Ivakhno, Fiz. Tverd. Tela (Leningrad) 14, 578 (1972) [Sov. Phys.—Solid State 14, 481 (1972)].

[47]J. Tauc and A. Abraham, Czech. J. Phys. 9, 95 (1959).

[48]C. Canali, M. Martini, G. Ottaviani, and A. Alberigi Quaranta, IEEE Trans. Nucl. Sci. NS-19, 9 (1972).

[49]With the assumption of uniform population, $\partial\epsilon/\partial E_g$ is $1+1.2E_{\rm th}/E_g$, i.e., 2.2 or 2.8 for $E_{\rm th}=E_g$ or $E_{\rm th}=1.5E_g$. With the scattering-rate assumption, $\partial\epsilon/\partial E_g$ and $\partial\bar{\epsilon}/\partial E_g$ are positive and increase with E_g, and their maximum values are 2.1 and 1.6, respectively.

[50]H. R. Bilger, Phys. Rev. 163, 238 (1967) [F(Ge) = 0.129 ± 0.003]; A. H. Sher and B. D. Pate, Nucl. Instrum. and Methods 71, 251 (1969) [F(Ge) = 0.132 ± 0.008]; H. R. Zulliger, J. Appl. Phys. 42, 5570 (1971) [F(Ge) = 0.063 ± 0.02, F(Si) = 0.087 ± 0.03]; Ref. 23 [F(Si) = 0.16 ± 0.04].

[51]An alternative form of Eq. (12) is

$$p_n(E)=\sum_{m=0}^{\infty}P_m(E)\,\frac{r_{n-1}(E-m\hbar\omega_0)}{r(E-m\hbar\omega_0)}\,.$$

This calculation was done by adopting the approximation of Ref. 12, that is, by replacing this equation with

$$p_n(E)\approx PI(E)r_{n-1}(E)/r(E)$$

which excludes phonon scattering losses for particles with energies above the final states.

[52]R. L. Platzman, Int. J. Appl. Radiat. Isot. 10, 116 (1961).

[53]See Eq. (2) of Ref. 52; the resemblance is increased when our Eq. (29) is integrated over all E'.

[54]W. M. Jones, J. Chem. Phys. 59, 5688 (1973).

[55]J. K. Knipp, T. Eguchi, M. Ohta, and S. Nagata, Prog. Theor. Phys. 10, 24 (1953); M. Inokuti, A. Douthat, and A. R. P. Rau, Bull. Am. Phys. Soc. 25, 37 (1980).

[56]J. M. Ziman, *Electrons and Phonons* (Oxford University Press, London, 1960).

[57]W. A. Harrison, Phys. Rev. 104, 1281 (1956).

[58]G. A. Baraff, Phys. Rev. 128, 2507 (1962).

[59]W. Shockley and H. J. Queisser, J. Appl. Phys. 32, 510 (1961).

[60]S. Deb and H. Saha, Solid-State Electron. 15, 1389 (1972); P. M. Dunbar and J. R. Hauser, *ibid.* 19, 95 (1976).
[61]B. Goldstein, J. Appl. Phys. 36, 3853 (1965).
[62]E. A. Konorova and S. F. Kozlov, Fiz. Tekh. Poluprovodn. 4, 1865 (1970) [Sov. Phys.—Semicond. 4, 1600 (1971)].
[63]G. P. Golubev, V. S. Vavilov, and V. D. Egorov, Fiz. Tverd. Tela (Leningrad) 7, 3702 (1965) [Sov. Phys.—Solid State 7, 3000 (1966)].
[64]P. J. van Heerden, Phys. Rev. 106, 468 (1957).
[65]W. Lehmann, J. Electrochem. Soc. 118, 1164 (1971).
[66]In CaS, $\epsilon_k(\hbar\omega_p)$ and $\bar{\epsilon}_k(\hbar\omega_p)$ differ by a factor of three because accidentally $\hbar\omega_p$ is slightly below $E_g + 2E_{th}$ and is slightly above $E_g + 2\bar{E}_{th}$. See Fig. 4 and the discussion ending Sec. IV A.